J Mater Sci (2017) 52:9430–9440

Chemical routes to materials

Amphiphilic polymer–drug conjugates based on acid-sensitive 100% hyperbranched polyacetals for cancer therapy

Xiao Duan[1], Yalan Wu[2], Mengsi Ma[1], Junjie Du[1], Shan Zhang[1], Heng Chen[1], and Jie Kong[1,*]

[1] MOE Key Laboratory of Space Applied Physics and Chemistry, Shaanxi Key Laboratory of Macromolecular Science and Technology, School of Science, Northwestern Polytechnical University, Xi'an 710072, People's Republic of China
[2] PLA No. 323 Hospital, Xi'an, Shaanxi Province 710054, People's Republic of China

Received: 4 March 2017
Accepted: 24 April 2017
Published online: 1 May 2017

ABSTRACT

A new type of acid-sensitive 100% hyperbranched polyacetals (HBPA) was synthesized, which could be completely degraded into small molecules under acidic environment and avoid the accumulative toxicity in vivo. The AB_2 monomer was synthesized by 4-carboxybenzaldehyde and 2-bromoethanol. The bulk polycondensation was carried out in vacuum environment to remove water byproduct. The massive terminal aldehyde groups of HBPA were conjugated with mPEG-NH_2 and doxorubicins to form amphiphilic acid-sensitive polymer–drug conjugates (DOX-HBPA-PEG). The stability of the micelles of DOX-HBPA-PEG was evaluated by DLS at different pH value in phosphate buffer saline (PBS). The DOX release in vitro showed that the cumulative release rate was 14.51% in pH 7.4 PBS after 24 h and the cumulative release rate was 48.56% in pH 6.0 PBS after 24 h. The results of cell viability of DOX-HBPA-PEG and HBPA-PEG showed that the polymer–DOX conjugates were effective drug delivery systems. The uptake process of DOX-HBPA-PEG by A549 cells showed that the micelle was totally swallowed in 1 h later. The controllable drug release nature, stability, biocompatibility and completely degradable structures (acid-sensitive) make them to be promising drug delivery systems.

Introduction

Nowadays, numerous drug delivery systems have been reported for delivering anticancer drugs to tumors based on inorganic carriers of mesoporous silica nanocapsules [1, 2], nanobubbles [3], carbon nanotubes [4, 5] and Au nanoparticles [6, 7] as well as organic carriers of nanoporous polymers [8], hyperbranched polymer [9], dendrimers [10], polymer–drug conjugates [11, 12] and polymer micelles [13]. Most of drug delivery systems are fabricated from polymers or macromolecules. The biocompatibility,

Address correspondence to E-mail: kongjie@nwpu.edu.cn

DOI 10.1007/s10853-017-1135-1

biodegradability and water solubility of polymers or macromolecules were usually evaluated before use. For drug delivery system, the macromolecules or polymers cannot pass through the endothelium of normal blood vessels [14]; at the same time, the metabolism and excretion are pretty hard for macromolecules or polymers. The rate of renal elimination is inversely correlated with the molecular weight of the polymers [15, 16]. The polymers need to be degraded into small molecules and excreted via kidney, otherwise resulting in accumulative toxicity in vivo. Conversely, the small molecules are delivered systemically and consequently exhibit a non-specific biodistribution, short plasma circulation times and rapid systemic elimination [17]. These properties avoid the accumulative toxicity in specific normal tissues of polymers or macromolecules.

The polymers or macromolecules used for drug delivery should be eliminated from the body, either by excretion of non-biodegradable polymers or by degradation of biodegradable polymers [18]. The backbones of biodegradable polymer usually are linked by ester bonds [19–22], ether bonds [23–27], carbon–carbon bonds [28, 29] and amide bonds [30, 31]. This type of polymer cannot be controllable and rapidly degraded into small molecules in target tissue or in vivo, resulting in long degradation time and accumulative toxicity to normal tissues in vivo. Although many drug delivery systems with partial stimulated bonds or polymer can respond to the change of environment, like temperature [32, 33], pH value [34, 35], light [36, 37], redox-reduction reagent [38, 39] and magnetic field [40, 41], most of polymers or macromolecules for drug delivery systems cannot be completely degraded into small molecules with partial stimulated linker bonds of disulfide bond [38, 42, 43], imine bond [29] and acetal bond [19, 42]. These linker bonds need to be repeat units in backbone of polymers or macromolecules for complete degradation. The backbone with pH or glutathione responsive bonds [44–47] can be completely degraded into small molecule in tumor cells because of the environment of tumor cells with low pH value and high concentration of glutathione.

The perfect polymers or macromolecules in drug delivery system for cancer therapy should be degraded into small molecule in the environment of low pH or high concentration of glutathione after delivering anticancer drugs to tumor cells. The polymers or macromolecules cannot freely pass through the cell membrane. Only small molecule drugs or monomer can freely pass through the cell membrane followed by blood stream to kidney to excrete via urinary tract. So the completely degradable polymers under low pH or glutathione can avoid the accumulative toxicity of polymers or macromolecules in vivo.

In this paper, we synthetized 100% hyperbranched polyacetals that can completely be degraded into monomers with aldehyde and hydroxyl groups in acidic environment in tumor cells. The hyperbranched polyacetals possess massive terminal aldehyde groups that can react with amino-terminated monopolyethylene glycol and DOX. The micelles of DOX-HBPA-PEG were characterized by NMR, FTIR, SEC and DLS. The properties of drug release and stability were evaluated in vitro, and the cell viability and uptake process were evaluated by A549 cell line in vitro.

Materials and methods

Materials

Doxorubicin hydrochloride (DOX·HCl) was purchased from Aladdin Co. (China). Amino-terminated monopolyethylene glycol (mPEG-NH_2, M_w = 2000 -Da) was purchased from Shanghai Yare Biotech, Inc. The 4-carboxybenzaldehyde and 2-bro-moethanol, *N*, *N*-dimethyl formamide (DMF) and tetrahydrofuran (THF) were purchased from J&K Scientific Ltd. (Beijing, China); CCK-8 and Hoechst Staining Kit were purchased from Beyotime company. The pyridinium camphorsulfonate (PCS) catalyst was synthesized using a similar protocol to the literature [46].

Characterization

Fourier transform infrared spectroscopy (FTIR) was performed on an MIR-NIR PerkinElmer, 1605 Series spectrophotometer using a diamond attenuated total reflectance accessory (ATR). Nuclear magnetic resonance (NMR) measurement was taken on a Bruker Avance 400 spectrometer (Bruker BioSpin, Switzerland) to collect the ^1H and ^{13}C spectra in DMSO-d_6. The average hydrodynamic radius of micelles was measured by using a Zetasizer ZEN 3500 dynamic light scattering (DLS) (Malvern instrument, UK). All DLS measurements were taken with an angle detection of 173° at 25 °C. All data were averaged over two measurements. All samples were filtered through

0.45-μm filters to remove dust prior to use. AUV-2450 UV–Vis spectrophotometer (Shimadzu, Japan) was used to determine the doxorubicin release rate of micelle DOX-HBPA-PEG. Size exclusion chromatography (SEC) measurement was taken on a system equipped a Waters 515 pump with a flow rate of 0.5 mL min^{-1} in THF (HPLC grade) at 25 °C. Detectors were including differential refractometer (OptilabrEX, Wyatt) and multiangle light scattering detector (MALLS) equipped with a 632.8 nm He–Ne laser (DAWN EOS, Wyatt). The refractive index increments of polymers in THF were measured at 25° Cusing an OptilabrEX differential refractometer. ASTRA software (version 5.1.3.0) was utilized for acquisition and analysis of data. Cell viability was detected by M200 Pro NanoQuant (TECAN). The cell uptake experiment was conducted by inverted fluorescence microscope (Olympus IX73).

Synthesis of AB_2 monomer 2-hydroxyethyl-4-formylbenzoate

The synthesis route of AB_2 is described in Scheme 1. The 4-carboxybenzaldehyde (5.00 g, 33.3 mmol), KOH (1.87 g, 33.3 mmol) and 2-bromoethanol (4.16 g, 33.3 mmol) were stirring overnight in 30 mL DMF under 100 °C with reflux condensation in round-bottom flask. The DMF was concentrated by evaporation under a reduced pressure; then, 100 mL ethyl acetate was added in DMF concentrated solution. The ethyl acetate organic solution was washed three times with $NaHCO_3$ and then washed three times with

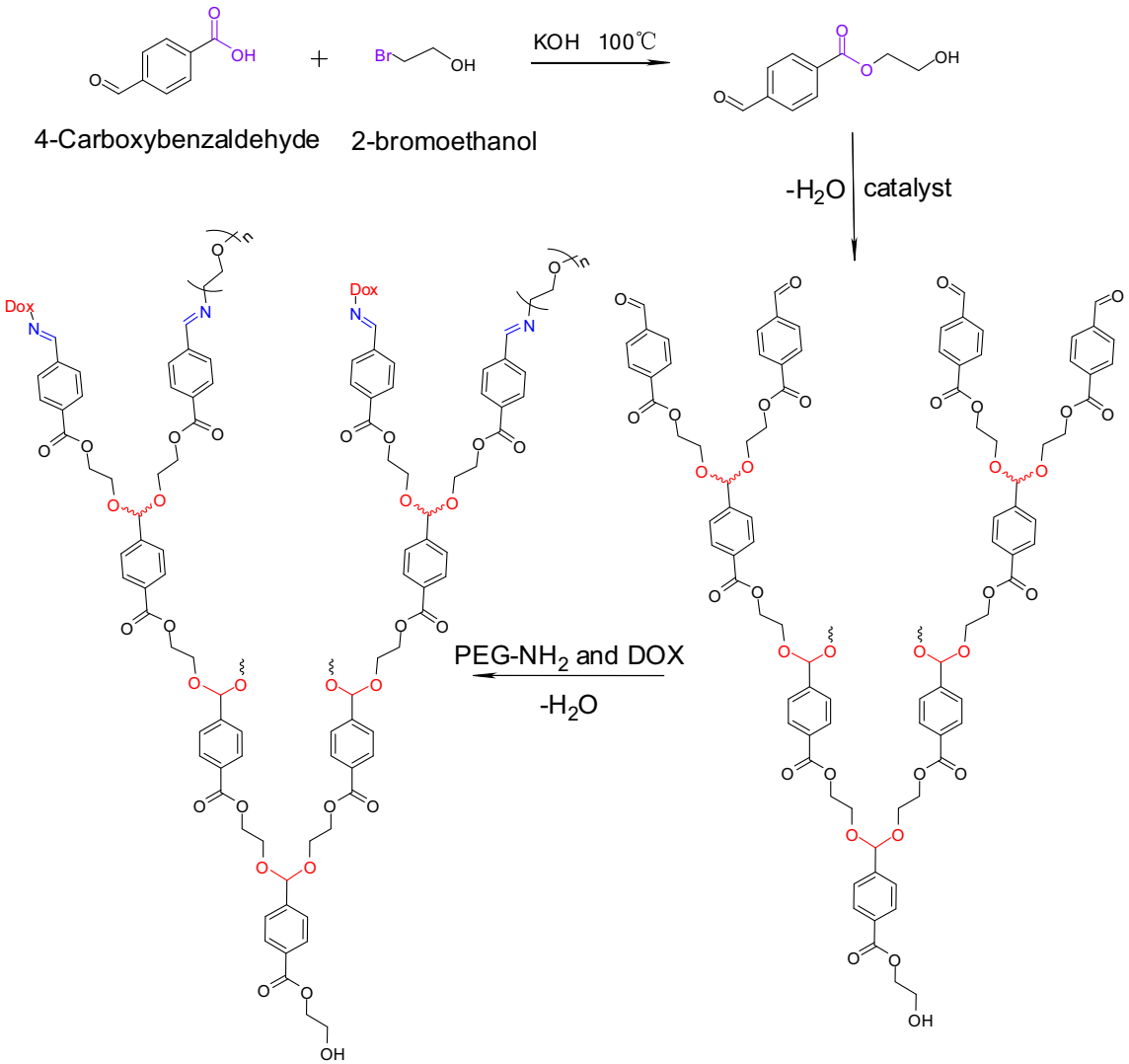

Scheme 1 The synthesis route of 100% hyperbranched polyacetals conjugated with PEG and DOX.

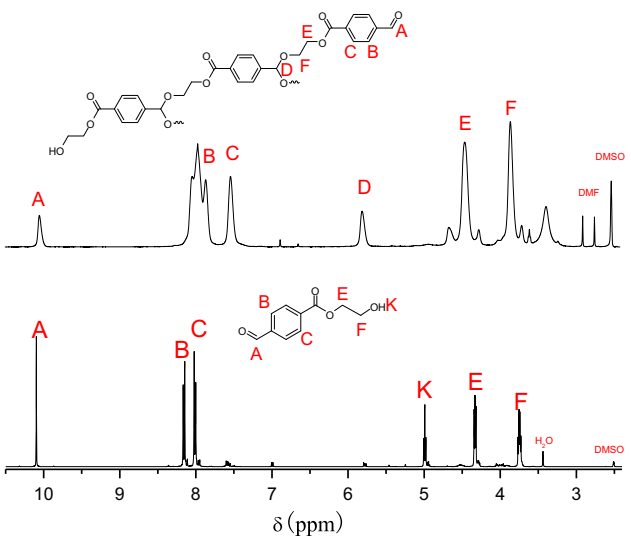

Figure 1 The ^{1}H NMR spectrum of hyperbranched polyacetals in DMSO-d_6.

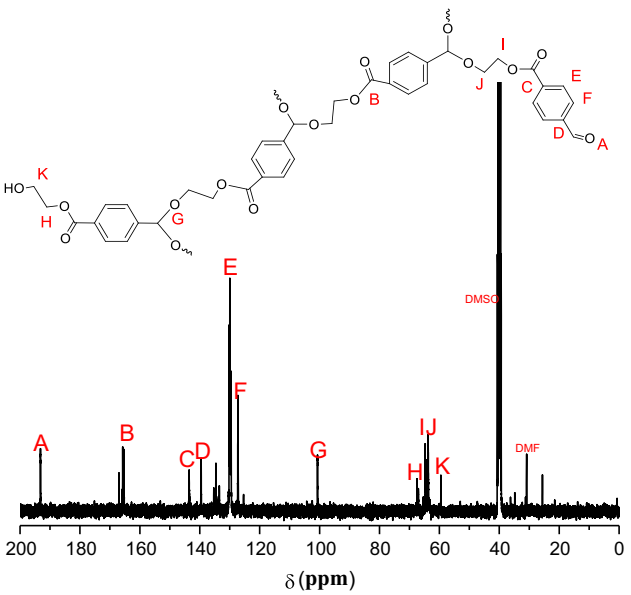

Figure 2 The ^{13}C NMR spectrum of hyperbranchedpolyacetals in DMSO-d^6.

pure water. The organic solution of ethyl acetate was concentrated under reduced pressure to yield the yellowish liquid. The yellowish liquid was purified by flash chromatography (1:1 hexane/EtOAc) to supply 3.7 g AB_2 monomer as clear oil (57% yield). IR (KBr): ν = 3449, 2960, 2837, 1707 cm^{-1}. ^{1}H NMR (400 MHz, DMSO-d_6, δ): 3.78 (t, 2H, –CH_2–), 4.42 (t, 2H, –CH_2–), 5.00 (s, 1H, –OH–), 8.00 (d, 1H, –CH–), 8.12 (d, 1H, –CH–), 10.12 (s, 1H, –CHO–).

Polymerization of AB_2 monomer to obtain 100% hyperbranched polyacetals

The polymerization reaction is shown in Scheme 1. AB_2 monomer 2-hydroxyethyl-4-formylbenzoate (3 g, 15.5 mmol) with 2% molpyridinium camphorsulfonate was added to Schlenk tube. The reaction was vacuum degassing three times and carried out in vacuum status under 60 °C. The polymerization reaction was carrying out under vacuum pumping interval 12 h to remove the water byproduct. Five days later, polyacetals were dissolved to 2 mL THF and then precipitated twice in methanol (78% yield, white solid). IR (KBr): ν = 3546, 2952, 2870, 1707 cm^{-1}. ^{1}H NMR (400 MHz, DMSO-d_6, δ): 3.86 (2H, –CH_2–), 4.45 (2H, –CH_2–), 5.80 (1H, –O–CH–O–), 7.56 (1H, –CH–), 8.00 (1H, –CH–), 10.02 (1H, –CHO–); ^{13}C NMR (400 MHz, DMSO-d_6, δ): 63.75, 65.28 (–CH_2–), 100.88 (–O–CH–O–), 127.00, 130.14 (ArCH), 165.18 (C=O), 192.80 (–CHO–).

PEGylation of hyperbranched polyacetals and synthesis of DOX-HBPA-PEG

HBPA (200 mg) and mPEG-NH_2 (100 mg) were dissolved in DCM (10 mL) in 25-mL round-bottom flask with Molecular Sieves. A few drops of acetic acid dropped in flask. The reaction was carried out at room temperature for 24 h. The reaction solution was put into dialysis bag (M_W = 3500) and then placed in ethanol. 12 h later, put the dialysis bag into water and change pure water three times. The solution of HBPA-PEG was freeze-dried powder (60% yield). IR (KBr): ν = 2874, 1707, 1640 (–CH=N–) cm^{-1}. ^{1}H NMR (400 MHz, DMSO-d_6, δ): 3.50 (4H, –CH_2CH_2O–), 3.86 (2H, –CH_2–), 4.45 (2H, –CH_2–), 5.80 (1H, –O–CH–O–), 7.56 (1H, –CH–), 8.00 (1H, –CH–), 8.36 (1H, –CH=N–), 10.02 (1H, –CH–); ^{13}C NMR (400 MHz, DMSO-d_6, δ): 63.75, 65.28 (–CH_2–), 100.88 (–O–CH–O–), 127.00, 130.14 (ArCH), 165.18 (C=O), 192.80 (–CHO–).

HBPA-PEG (130 mg) and DOX·HCl (25 mg) were dissolved in DCM (10 mL) in 25-mL round-bottom flask with Molecular Sieves. The reaction was carried out at room temperature for 24 h. The reaction solution was put into dialysis bag (M_W = 3500) and then placed in DMF and change three times DMF solvent. 24 h later, put the dialysis bag into water and change pure water three times. The micelle solution of DOX-HBPA-PEG was reassembled by centrifugalization; then, the supernatant was freeze-dried red powder.

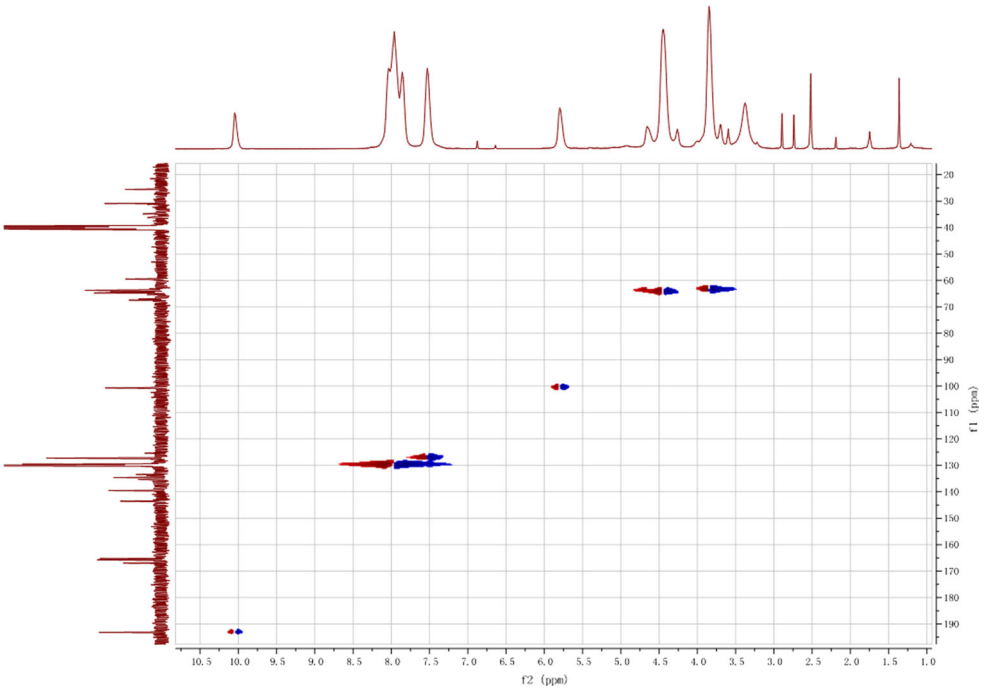

Figure 3 The ^{13}C–^{1}H COSY spectrum of hyperbranched polyacetals in DMSO-d_6.

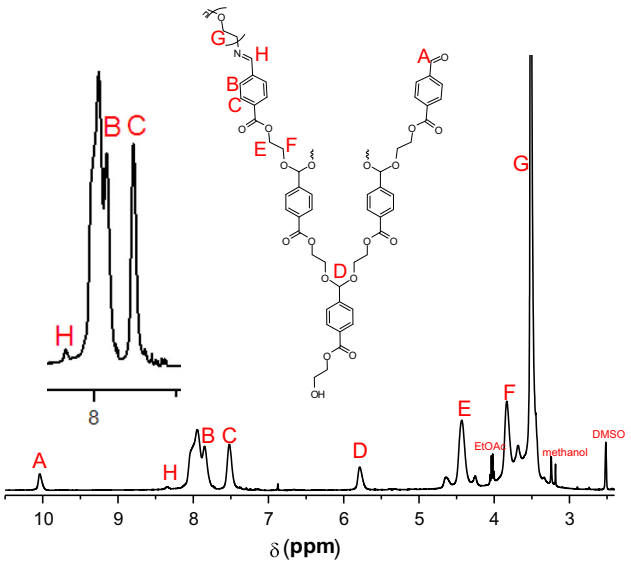

Figure 4 The ^{1}H NMR spectrum of HBPA-PEG in DMSO-d_6.

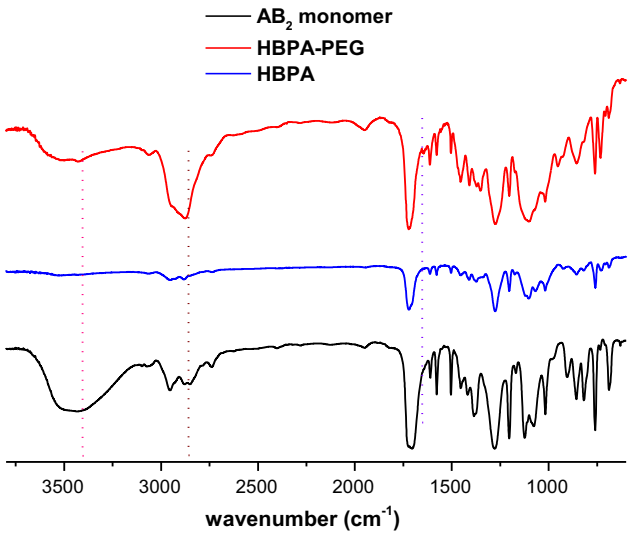

Figure 5 The FTIR spectra of HBPA-PEG, HBPA and AB_2 monomer.

Evaluation of stability, drug release of DOX-HBPA-PEG and drug loading

The freeze-dried red powder of DOX-HBAP-PEG (9 mg) was solubilized in pH 6.0 and pH 7.4 PBS, respectively. The micelle of DOX-HBAP-PEG (3 mg mL^{-1}) was centrifuged, and the supernatant was evaluated with the time passing at the condition of pH 6.0 and pH 7.4 PBS. The drug release rate of DOX from the micelle of DOX-HBAP-PEG was measured by UV–Vis spectrophotometer at 496 nm. The four parts of 3 mL micelle solution with pH 7.4 PBS were put into dialysis bag ($M_W = 1000$); then, the dialysis bags were put into pH 6.0 and pH 7.4 PBS, respectively. 3 mL dialysis solution outside dialysis bag was taken out at every interval time; then, add 3 mL fresh PBS to dialysis solution. The eight solution samples which were taken out from solution outside dialysis bag at eight points-in-time were prepared to be measured. The experiments

Table 1 The molecular weight of HBPA and HBPA-PEG

Sample	M_w (g mol^{-1})	M_n (g mol^{-1})	PDI
HBPA	9100	6300	1.46
HBPA-PEG	13900	10400	1.34

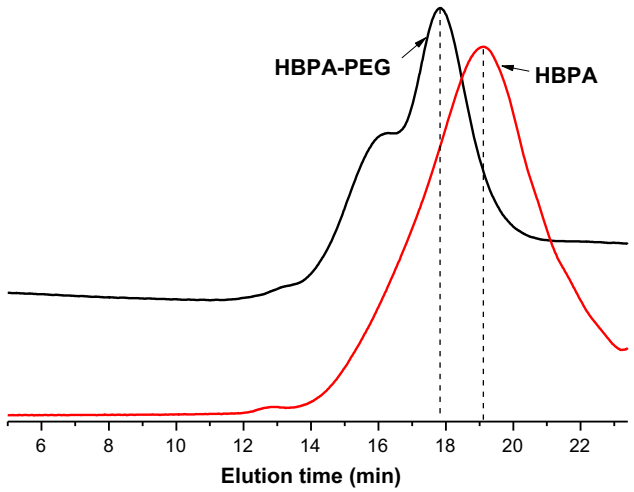

Figure 6 The elution time (t)-dependent SEC-RI curves of polymer HBPA and HBPA-PEG with a flow rate of 0.5 mL min^{-1} in THF.

were carried out twice in parallel. The drug loading is 12% measured by UV–Vis spectrometer at 496 nm.

Cell viability in vitro

The cell viability of DOX-HBPA-PEG and HBPA-PEG was evaluated using the Cell Counting Kit (CCK-8) assay. The concentrations of DOX in micelle of DOX-HBPA-PEG were 1, 5, 10 μg mL^{-1}, and the concentrations of HBPA-PEG were 56, 112, 280 μg mL^{-1}, respectively. The Lung A549 cells were seeded in a 96-well culture plate at a density of 10^4 cells per well and cultured in DMEM medium supplemented with 10% fetal bovine serum at 37 °C in a humidified environment of 5% CO_2 for 1 day. Thereafter, the cells were incubated with DOX-HBPA-PEG and HBPA-PEG for 24 and 48 h, respectively. 10 μL of CCK-8 solution was added to each well and incubated for further 1 h at 37 °C. The cell viability was obtained by scanning with a microplate reader at 430 nm. The relative cell viability (%) was expressed as a percentage of that of the control culture. The experiments were carried out six times in parallel. The results presented are the average data.

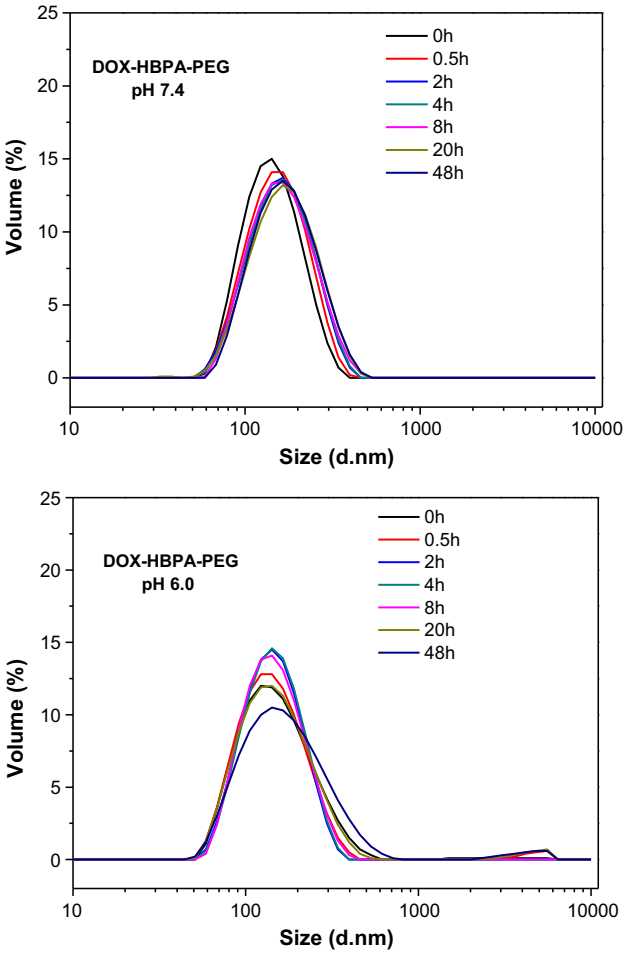

Figure 7 The stability with time passing of DOX-HBPA-PEG in PBS at different pH.

Table 2 The size of DOX-HBPA-PEG measured by dynamic light scattering in PBS

DOX-HBPA-PEG				
Time (h)	pH 6.0		pH 7.4	
	Size (d.nm)	PDI	Size (d.nm)	PDI
4	133	0.134	148	0.136
20	136	0.187	154	0.121
48	152	0.228	156	0.152

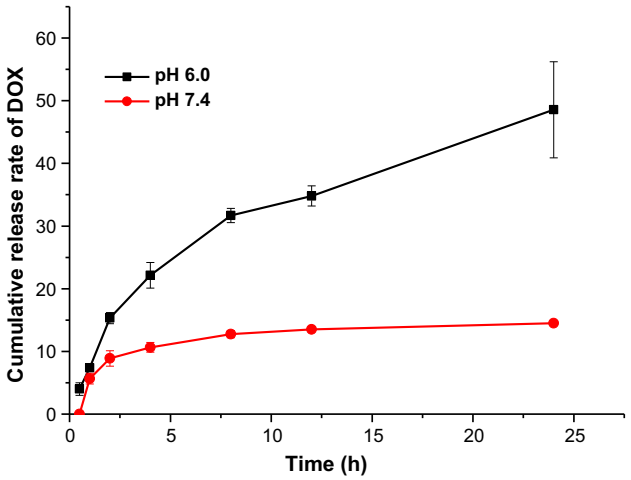

Figure 8 The cumulative release rate of DOX from the micelle of DOX-HBPA-PEG in PBS at the conditions of pH 7.4 and pH 6.0 (the experiments were carried out twice in parallel).

Cellular uptake assay

Lung A549 cells were seeded with a density of 5×10^4 per dish in 35 mm plastic microscopy dishes and incubated overnight at 37 °C. Then, the A549 cells were treated with 0.25 mg mL^{-1} DOX-HBPA-PEG micelles for 0 min, 15 min, 1 h, 4 h, respectively. Then, the cells were fixed and stained by Hoechst Staining Kit for 10 min, respectively, then gently rinsed with PBS three times and observed with fluorescence microscope.

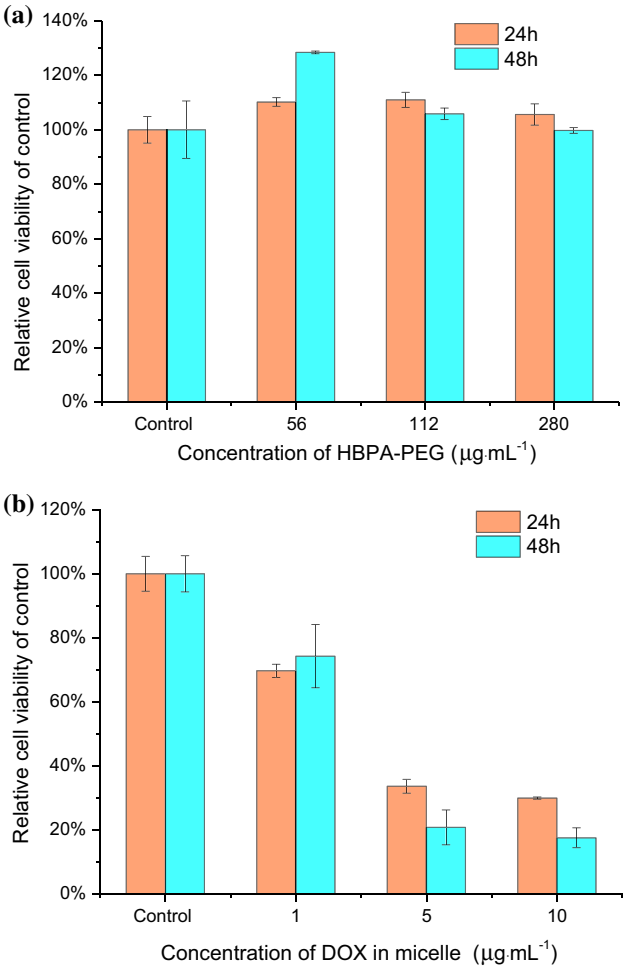

Figure 9 The cell viability of **a** HBPA-PEG (56, 112, 280 μg mL^{-1}) and **b** DOX-HBPA-PEG micelle (8.3, 41.7, 83.3 μg mL^{-1}) with different concentration at 24 and 48 h later.

Results and discussion

Synthesis of AB_2 monomer 2-hydroxyethyl-4-formylbenzoate and 100% hyperbranched polyacetals

The synthesis route of AB_2 and 100% hyperbranched polyacetals is described in Scheme 1. The characteristic peak of –CHO– is showed at 10.12 ppm by ^1H NMR (Fig. 1) and the characteristic peak of –OH at the wavenumber 3449 cm^{-1} by IR spectrum. The crude material of 4-carboxybenzaldehyde can be washed out by $NaHCO_3$ water solution; then, the product was purified by flash chromatography (1:1 hexane/EtOAc) to obtain pure AB_2 monomer for polycondensation reaction. The reaction of AB_2 monomers was catalyzed by PCS in bulk polymerization. The molar masses of polyacetalization are increased as the removing the water byproduct. The product of polyacetals was characterized by ^1H, ^{13}C NMR spectra. The polyacetals characteristic peak of OH obviously decreased compared to AB_2 monomer, meaning the acetal bond is continuously forming. The acetal bonds are particular structure for the polymer of polyacetals. The characteristic peak of –O–CHO– is 5.80 ppm in ^1H NMR, and the characteristic peak of –O–CHO– is 100.88 ppm in ^{13}C NMR (Figs. 1, 2). The structure of polyacetals further confirmed by using 2D ^{13}C–^1H COSY spectra. The cross dot of 100.88 ppm in ^{13}C NMR and 5.80 ppm in ^1H NMR in Fig. 3 means the C–H correlation peak of acetals (–O–C–O–).

PEGylation of hyperbranched polyacetals

The hyperbranched polyacetals were characterized by NMR and FTIR. The signal of aldehyde proton (10.02 ppm) is decreased, and the signal of imine bond proton (8.36 ppm) clearly appeared, meaning the PEG was conjugated with HBPA (Fig. 4). The FTIR also demonstrated the imine bond (1640 cm^{-1}) is formed. The characteristic peak of –OH in HBPA is disappeared, and the characteristic peak of imine bond in HBPA-PEG is appeared (Fig. 5). The molecular weight of HBPA-PEG and HBPA in Table 1 showed that two mPEG-NH_2 molecules at least were conjugated with HBPA. The shoulder peak further confirms that more molecules of mPEG-NH_2 were conjugated with HBPA (Fig. 6 and Table 1).

The stability of DOX-HBPA-PEG

The amphiphilic polymer of DOX-HBPA-PEG was evaluated by DLS in pH 7.4 and pH 6.0 PBS at different time. The size of DOX-HBPA-PEG did not remarkable change over time at pH 7.4 PBS. To simulate the tumor extracellular environment, we evaluated the stability of micelle of DOX-HBPA-PEG in pH6.0 PBS. Figure 7 showed the micelle display

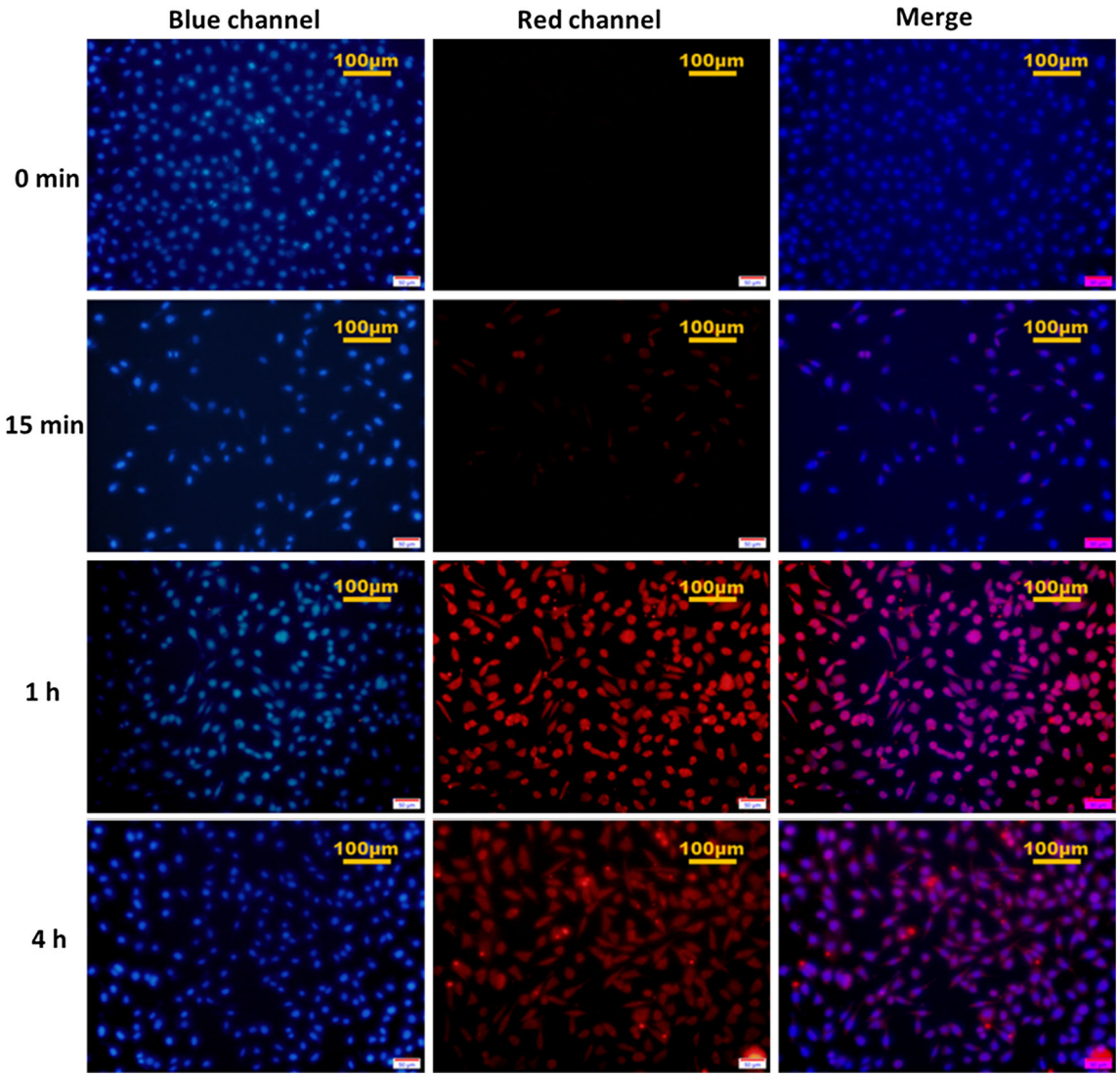

Figure 10 Investigation of DOX-HBPA-PEG endocytosis by A549 cell at different time (*blue channel*: nucleuses were dyed by Hoechst 33258, *red channel*: DOX-HBPA-PEG).

the double peak and the distribution is broader in pH 6.0 PBS. The results of DOX-HBPA-PEG measured by dynamic light scattering (Table 2) further confirmed that the micelle of DOX-HBPA-PEG was stable in pH7.4 PBS. The data in Table 2 showed that the polydispersity index (PDI) and size of the micelle of DOX-HBPA-PEG obviously increased with the time passing in pH 6.0 PBS and the PDI and size of the micelle of DOX-HBPA-PEG did not clearly change with the time passing in pH 7.4 PBS. It means the micelle of DOX-HBPA-PEG was disrupted in acidic environment and stable in physiological environment in vivo.

Drug release of DOX-HBPA-PEG

The drug release property of DOX-HBPA-PEG was evaluated at the condition of pH 7.4 and pH 6.0 in PBS (Fig. 8). The micelle of DOX-HBPA-PEG was stable in pH 7.4 PBS, and the drug release rate is 14% 24 h later. The micelle of DOX-HBPA-PEG was unstable in pH 6.0 PBS, and the drug release rate is 48% 24 h later. The results of accumulated drug release rate in pH 7.4 and pH 6.0 PBS showed the drug of DOX was controllable released in acidic environment.

Cell viability of HBPA-PEG and DOX-HBPA-PEG in vitro

The cell viability of HBPA-PEG and DOX-HBPA-PEG was evaluated by A549 cells in vitro at 24 and 48 h later. The cell viability of HBPA-PEG with different concentration did not change. The results of Fig. 9a illustrated that the biocompatibility of HBPA-PEG was pretty good, even the highest concentration of HBPA-PEG is 280 μg mL^{-1}. The decreased cell viability of DOX-HBPA-PEG was typically responsive to the increased DOX concentrations in micelle (Fig. 9b). The results of cell viability in Fig. 9 illustrated the polymer of HBPA-PEG have no toxicity compared to polymer–drug conjugate of DOX-HBPA-PEG at the same concentration. It means the cell apoptosis was triggered by DOX.

Cellular uptake assay

To investigate the distribution of micelle of DOX-HBPA-PEG in A549 cells, the nucleus were dyed by Hoechst 33258 at 0 min, 15 min, 1 h, 4 h, respectively, after being treated with 0.25 mg mL^{-1} DOX-HBPA-PEG. The micelle of DOX-HBPA-PEG was swallowed slightly by A549 cells at 15 min later in red channel and merge channel. One hour later, the micelle of DOX-HBPA-PEG totally overlapped with nucleus in merge channel. These results in Fig. 10 further confirmed that the cell apoptosis was triggered by DOX.

Conclusions

Hyperbranched polyacetals is an acidic-sensitive polymer which can completely degrade into small molecule in acidic environment. We adopted a simple method to synthesize the 100% hyperbranched polyacetals. The AB_2 monomer 2-hydroxyethyl-4-formylbenzoate was catalyzed by PCS with bulk polymerization. The polymerization products of polyacetals were modified by PEG-NH_2 to form amphiphilic polymer for drug delivery system. The synthesis route was characterized by ^{1}H, ^{13}C NMR, ^{13}C–^{1}H COSY spectra and FTIR spectrum. The terminal aldehyde groups of polyacetals were conjugated with DOX to form acidic-sensitive imine bonds. The micelle of DOX-HBPA-PEG was very stable in pH 7.4 PBS, and the DOX can be controllable released at pH 6.0 PBS. The results of cell viability and uptake confirm that the micelle of DOX-HBPA-PEG is an effective drug delivery system for cancer therapy. The controllable drug release nature, stability, biocompatibility and completely degradable structures (acid-sensitive) make them to be promising drug delivery systems.

Acknowledgements

The financial support from National Natural Science Foundation of China (21374089/81400765) is acknowledged.

Compliance with ethical standards

Conflict of interest The authors declare that they have no conflict of interest.

References

[1] Zhang P, Cheng F, Zhou R, Cao J, Li J, Burda C, Min Q, Zhu J (2014) DNA-hybrid-gated multifunctional mesoporous

silica nanocarriers for dual-targeted and microRNA-responsive controlled drug delivery. Angew Chem Int Ed 126:2403–2407

[2] Ma M, Huang Y, Chen H, Jia X, Wang S, Wang Z, Shi J (2015) Bi_2S_3-embedded mesoporous silica nanoparticles for efficient drug delivery and interstitial radiotherapy sensitization. Biomaterials 37:447–455

[3] Geers B, Dewitte H, De Smedt SC, Lentacker I (2012) Crucial factors and emerging concepts in ultrasound-triggered drug delivery. J Control Release 164:248–255

[4] Soldano C (2015) Hybrid metal-based carbon nanotubes: Novel platform for multifunctional applications. Prog Mater Sci 69:183–212

[5] Chen P, Hsiao KM, Chou C (2013) Molecular characterization of toxicity mechanism of single-walled carbon nanotubes. Biomaterials 34:5661–5669

[6] Fan L, Campagnoli S, Wu H, Grandi A, Parri M, Camilli ED, Grandi G, Viale G, PileriP Grifantini R, Song CJ, Jin B (2015) Negatively charged AuNP modified with monoclonal antibody against novel tumor antigen FAT1 for tumor targeting. J Exp Clin Cancer Res 34:103

[7] Fan L, Zhang YS, Wang F, Yang Q, Tan J, Grifantini R, Wu H, Song CJ, Jin B (2016) Multifunctional all-in-one drug delivery systems for tumor targeting and sequential release of three different anti-tumor drugs. Biomaterials 76:399–407

[8] Amiri A, Ramazani A, Jahanshahi M, Moghadamnia AA (2016) Synthesis and evaluating of nanoporous molecularly imprinted polymers for extraction of quercetin as a bioactive component of medicinal plants, Iran. J Chem Chem Eng 35(4):11–19

[9] Malekzadeh AM, Ramazani A, Rezaei SJT, Niknejad H (2017) Design and construction of multifunctional hyperbranched polymers coated magnetite nanoparticles for both targeting magnetic resonance imaging and cancer therapy. J Colloid Interface Sci 490:64–73

[10] Dayyani N, Khoee S, Ramazani A (2015) Design and synthesis of pH-sensitive polyamino-ester magnetodendrimers: surface functional groups effect on viability of human prostate carcinoma cell lines DU145. Eur J Med Chem 98:190–202

[11] QiaoYB Duan X, Fan L, Li W, Wu H, Wang YK (2014) Synthesis of controlled molecular weight poly (β-malic acid) and conjugation with HCPT as a polymeric drug carrier. J Polym Res 21:397–405

[12] Li F, Zhang HT, Gu CH, Fan L, QiaoYB Tao YC, Cheng C, Wu H, Yi J (2013) Self-assembled nanoparticles from folate-decorated maleilated pullulan–doxorubicin conjugate for improved drug delivery to cancer cells. Polym Int 62:165–171

[13] Li F, Fan L, Li W, Duan X, QiaoYB WuH (2014) Synthesis and micellar characterization of luteinizing hormone-releasing hormone poly(ethylene glycol)- block-poly(L-histidine) copolymers. Polym Eng Sci 55(2):277–286

[14] Fang J, Nakamura H, Maeda H (2011) The EPR effect: unique features of tumor blood vessels for drug delivery, factors involved, and limitations and augmentation of the effect. Adv Drug Deliv Rev 63:136–151

[15] Tetsuji Y, Yasuhiko T, Yoshito I (1994) Distribution and tissue uptake of poly(ethylene glycol) with different molecular weights after intravenous administration to mice. J Pharm Sci-US 84:601–606

[16] Tetsuji Y, Yasuhiko T, Yoshito I (1995) Fate of water-soluble polymers administered via different routes. J Pharm Sci-US 84:349–354

[17] Martin EE, Sebastian S, Marc D (2004) Anti-vascular tumor therapy: recent advances, pitfalls and clinical perspectives. Drug Resist Update 7:125–138

[18] Markovsky E, Baabur-Cohen H, Eldar-Boock A, Omer L, Tiram G, Ferber S, Ofek P, Polyak D, Scomparin A, Satchi-Fainaro R (2012) Administration, distribution, metabolism and elimination of polymer therapeutics. J Control Release 161:446–460

[19] Hong BJ, Chipre AJ, Nguyen ST (2013) Acid-degradable polymer-caged lipoplex (PCL) platform for siRNA delivery: facile cellular triggered release of siRNA. J Am Chem Soc 135:17655–17658

[20] Kumar A, Lale SV, Mahajan S, Choudhary V, Koul V (2015) ROP and ATRP fabricated dual targeted redox sensitive polymersomes based on pPEGMA-PCL-ss-PCL-pPEGMA triblock copolymers for breast cancer therapeutics. ACS Appl Mater Interfaces 7:9211–9227

[21] Sitia L, Ferrari R, Violatto MB, Talamini L, Dragoni L et al (2016) Fate of PLA and PCL-based polymeric nanocarriers in cellular and animal models of triple-negative breast cancer. Biomacromol 17:744–755

[22] Man DKW, Casettari L, Cespi M, Bonacucina G, Palmieri GF et al (2015) Oleanolic acid loaded PEGylated PLA and PLGA nanoparticles with enhanced cytotoxic activity against cancer cells. Mol Pharm 12:2112–2125

[23] Nascimento AV, Singh A, Bousbaa H, Ferreira D, Sarmento B et al (2015) Combinatorial-designed epidermal growth factor receptor-targeted chitosan nanoparticles for encapsulation and delivery of lipid-modified platinum derivatives in wild-type and resistant non-small-cell lung cancer cells. Mol Pharm 12:4466–4477

[24] Ferreira DP, Conceição DS, Fernandes F, Sousa T, Calhelha RC et al (2016) Characterization of a squaraine/chitosan system for photodynamic therapy of cancer. J Phys Chem B 120:1212–1220

[25] Kiani M, MirzazadehTekie FS, Dinarvand M, Soleimani M, Dinarvand R et al (2016) Thiolatedcarboxymethyl dextran as

a nanocarrier for colon delivery of hSET1 antisense: in vitro stability and efficiency study. Mater Sci Eng C-Mater 62:771–778

[26] Anirudhan TS, Binusreejayan (2016) Dextran based nano-sized carrier for the controlled and targeted delivery of curcumin to liver cancer cells. Int J Biol Macromol 88:222–235

[27] Tarvirdipour S, Vasheghani-Farahani E, Soleimani M, Bardania H (2016) Functionalized magnetic dextran-spermine nanocarriers for targeted delivery of doxorubicin to breast cancer cells. Int J Pharm 501:331–341

[28] Tomalova B, Sirova M, Rossmann P, Pola R, Strohalm J et al (2016) The structure-dependent toxicity, pharmacokinetics and anti-tumour activity of HPMA copolymer conjugates in the treatment of solid tumours and leukaemia. J Control Release 223:1–10

[29] Mao J, Li Y, Wu T, Yuan C, Zeng B et al (2016) A simple dual-pH responsive prodrug-based polymeric micelles for drug delivery. ACS Appl Mater Interfaces 8:17109–17117

[30] Zhang Y, Xiao C, Ding J, Li M, Chen X et al (2016) A comparative study of linear, Y-shaped and linear-dendritic methoxy poly(ethylene glycol)-block-polyamidoamine-block-poly(L-glutamic acid) block copolymers for doxorubicin delivery in vitro and in vivo. Acta Biomater 40:243–253

[31] Chen P, Qiu M, Deng C, Meng F, Zhang J et al (2015) pH-responsive chimaericpepsomes based on asymmetric poly(ethyleneglycol)-b-poly(L-leucine)-b-poly(L-glutamic acid) triblock copolymer for efficient loading and active intracellular delivery of doxorubicin hydrochloride. Biomacromolecules 16:1322–1330

[32] Chen FM, Lu H, Wu LA, Gao LN, An Y et al (2013) Surface-engineering of glycidylmethacrylated dextran/gelatin microcapsules with thermo-responsive poly(N-isopropylacrylamide) gates for controlled delivery of stromal cell-derived factor-1α. Biomaterials 34:6515–6527

[33] Li F, Wu H, Fan L, Zhang HT, Zhang H, Gu CH (2009) Study of dual responsive poly[(maleilated dextran)-graft-(N-isopropylacrylamide)] hydrogel nanoparticles: preparation, characterization and biological evaluation. Polym Int 58:1023–1033

[34] Fan L, Li F, Zhang HT, Wang YK, Cheng C, Li XY, Gu CH, Yang Q, Wu H, Zhang SY (2010) Co-delivery of PDTC and doxorubicin by multifunctional micellar nanoparticles. Biomaterials 31:5634–5642

[35] Wu H, Zhu L, Torchilin VP (2013) pH-sensitive poly(histidine)-PEG/DSPE-PEG co-polymer micelles for cytosolic drug delivery to achieve active targeted drug delivery and overcome multidrug resistance. Biomaterials 34:1213–1222

[36] Li DD, Wang JX, Ma Y, Qian HS, Wang D, Wang L, Zhang GB, QiuLZ Wang YC, Yang XZ (2016) A donor–acceptor conjugated polymer with alternating isoindigo derivative and bithiophene units for near-infrared modulated cancer thermo-chemotherapy. ACS Appl Mater Interfaces 8:19312–19320

[37] Wang JX, Liu Y, Ma YC, Sun CY, Tao W, Wang YC, Yang XZ, Wang J (2016) NIR-activated supersensitive drug release using nanoparticles with a flow core. Adv Funct Mater 26:7516–7525

[38] Zhang S, Chen H, Kong J (2016) Disulfide bonds-containing amphiphilic conetworks with tunable reductive-cleavage. RSC Adv 6:36568–36575

[39] Duan X, Chen H, Fan L, Kong J (2016) Drug self-assembled delivery system with dual responsiveness for cancer chemotherapy. ACS Biomater Sci Eng 2:2347–2354

[40] Dayyani N, Ramazani A, Khoee S, Shafiee A (2017) Synthesis and characterization of the first generation of poly-amino-ester dendrimer-grafted magnetite nanoparticles from 3-aminopropyltriethoxysilane (APTES) via the convergent approach. Silicon 12:1–7

[41] Tarasi R, Khoobi M, Niknejad H, Ramazani A, Ma'mani L, Bahadorikhalili S, Shafiee A (2016) β-Cyclodextrin functionalized poly(5-amidoisophthalicacid) grafted Fe_3O_4 magnetic nanoparticles: a novel biocompatible nanocomposite for targeted docetaxel delivery. J Magn Magn Mater 417:451–459

[42] An X, Zhu A, Luo H, Ke H, Chen H et al (2016) Rational design of multi-stimuli-responsive nanoparticles for precise cancer therapy. ACS Nano 10:5947–5958

[43] Talelli M, Vicent MJ (2014) Reduction sensitive poly(L-glutamic acid) (PGA)-protein conjugates designed for polymer masked-unmasked protein therapy. Biomacromolecules 15:4168–4177

[44] Liu N, Vignolle J, Vincent J-M, Robert F, Landais Y et al (2014) One-pot synthesis and PEGylation of hyperbranched polyacetals with a degree of branching of 100%. Macromolecules 47:1532–1542

[45] Parmar RG, Busuek M, Walsh ES, Leander KR, Howell BJ et al (2013) Endosomolytic bioreducible poly(amido amine disulfide) polymer conjugates for the in vivo systemic delivery of siRNA therapeutics. Bioconjug Chem 24:640–647

[46] Saptarshi C, Ramakrishnan S (2011) Hyperbranched polyacetals with tunable degradation rates. Macromolecules 44:4658–4664

[47] Chen H, Jia J, Duan X, Yang Z, Kong J (2015) Reduction-cleavable hyperbranched polymers with limited intramolecular cyclization via click chemistry. J Polym Sci PolChem 53:2374–2380